Full-wave verification of the fundamental properties of left-handed materials in waveguide configurations

C. Caloz,[a] C.-C. Chang, and T. Itoh
Electrical Engineering Department, University of California, Los Angeles, Los Angeles, California 90095

(Received 22 June 2001; accepted for publication 10 August 2001)

The fundamental electromagnetic properties of left-handed materials (LHMs) are reviewed and verified by finite-element method full-wave analysis using rectangular waveguide structures loaded by a LHM and adopting an effective medium approach. The negative phase velocity, positive intrinsic impedance, and modified boundary conditions at an interface with a right-handed medium are verified by loading a waveguide section with a LHM that has edges perpendicular to the waveguide axis. In addition, the negative angle of refraction is demonstrated by loading the junction of a *T*-junction waveguide with a LHM having one edge 45° with respect to the waveguide axis. These properties are shown by the evolution of wave fronts in the LHM and by analysis of the *S*-parameters of the waveguide structures. © *2001 American Institute of Physics.*
[DOI: 10.1063/1.1408261]

I. INTRODUCTION

Back in 1968, Veselago theoretically investigated materials with simultaneously negative permittivity and permeability, or left-handed materials (LHMs), and pointed out some of their electrodynamic properties, such as the reversal of Snell's law, the Doppler effect, and Cerenkov radiation.[1] But his idea was forgotten because of the unavailability of LHMs at that time. Recently, Pendry *et al.* discovered a microwave-plasma thin-wire structure exhibiting negative permittivity below the electronic plasma frequency[2] and a magnet-free split-ring resonator structure exhibiting negative permeability below the magnetic plasma frequency.[3] Soon afterwards, the first experimental demonstration of a LHM resulting from a combination of these two structures was given by Shelby *et al.*[4] Although still at the prototype stage, LHMs can potentially be applied to practical optical/microwave applications. An immense variety of novel applications, including new types of beam steerers, modulators, band-pass filters, superlenses,[5] microwave couplers, and antenna radoms, should be developed in the near future. In this article we review the fundamental electromagnetic properties of LHMs and provide a full-wave demonstration of these properties using the finite-element method (FEM) in LHM-loaded rectangular waveguide structures.

II. FUNDAMENTAL ELECTROMAGNETIC PROPERTIES OF LHMs

In a LH medium ($\varepsilon<0,\mu<0$), Maxwell's equations take the following form for a plane wave $[\mathbf{E}(\mathbf{r}),\mathbf{H}(\mathbf{r})]=[\mathbf{E}_0\mathbf{e}^{-\mathbf{jk}\cdot\mathbf{r}},\mathbf{H}_0\mathbf{e}^{-\mathbf{jk}\cdot\mathbf{r}}]$:

$$\mathbf{k}\times\mathbf{E}=-\omega|\mu|\mathbf{H}$$

and

$$\mathbf{k}\times\mathbf{H}=+\omega|\varepsilon|\mathbf{E}, \tag{1}$$

where the time dependence $e^{+j\omega t}$ is assumed. Consequently, the triplet (**E**, **H**, **k**) builds a *left-handed triad*, as illustrated in Fig. 1. Thus, the wave vector **k**, and therefore also the phase velocity $\mathbf{v}_\varphi$, exhibit *a sign opposite* to that in a conventional right-handed (RH) medium. At the same time, the Poynting theorem is still given by

$$\mathbf{S}=\mathbf{E}\times\mathbf{H}^*, \tag{2}$$

which indicates that the triplet (**E**, **H**, **S**) still builds a *right-handed triad*, also shown in Fig. 1. Thus, the Poynting vector **S**, and therefore also the group velocity $\mathbf{v}_{\mathbf{gr}}$, point in the same direction as the propagation of energy, as in a RH medium, thereby satisfying the causality requirement. Combining observations of the directions of **k** and **S** demonstrates that in a LHM the phase and group velocities are *antiparallel* (of opposite signs) and that the wave fronts travel *toward the source*.

The general time/space dependency of a plane wave is of the form $E,H\propto e^{+j(\omega t-nk_0r)}$, where $k_0r=(\omega/c_0)r>0$ if we define a system in which **r** is parallel to and pointing in the same direction as **S** (Fig. 1). Now, since we know from the above considerations that the wave is of an *incoming* nature

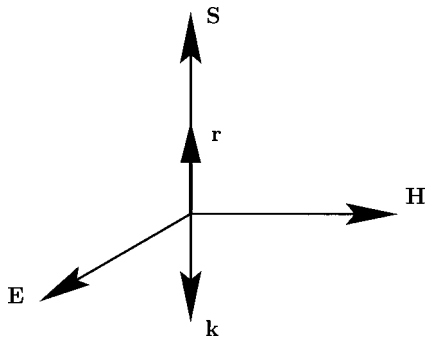

FIG. 1. Directions of the triads (**E**, **H**, **k**) and (**E**, **H**, **S**) in a LHM.

[a]Electronic mail: caloz@ee.ucla.edu

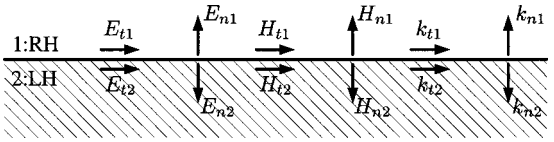

FIG. 2. Boundary conditions at an interface of RH/LH.

in the LH, nk_0r must be negative to yield the incoming wave expression $e^{+j(\omega t+|n|k_0r)}$, and therefore *the refractive index is negative* in a LHM,

$$n=-\sqrt{\varepsilon_r\mu_r}<0. \tag{3}$$

Let us examine now what happens to the boundary conditions (BCs) at the interface between a RH and a LH medium. The *tangential* (t) components of **E**, **H**, and **k** do not "see" the discontinuity and are therefore unaffected. In contrast, the *normal* (n) components of the same vectors undergo a *change of sign* (in addition to the magnitude discontinuity) at the interface. The change of sign for E_n and H_n comes directly from the conditions $\varepsilon_1E_{1n}=\varepsilon_2E_{2n}$ (with $\varepsilon_2<0$) and $\mu_1H_{1n}=\mu_2H_{2n}$ (with $\mu_2<0$), respectively, whereas the change of sign for k_n is a consequence of Eq. (3). The new BCs are summarized in Fig. 2.

After observing that the refractive index is negative in a LHM, we need to determine the sign of the intrinsic impedance η in such a medium. To do this, we consider a wave incident on a RH/LH interface, as shown in Fig. 3. In the case of $(\varepsilon_{r\mathrm{LH}},\mu_{r\mathrm{LH}})=-(\varepsilon_{r\mathrm{RH}},\mu_{r\mathrm{RH}})$, we expect *perfect matching* since the energy is the same in each medium. Therefore, the reflection coefficient at the interface must be zero, that is, for normal incidence ($\theta_i=0$), $\Gamma=(\eta_{\mathrm{LH}}-\eta_{\mathrm{RH}})/(\eta_{\mathrm{LH}}+\eta_{\mathrm{RH}})=0$ or $\eta_{\mathrm{LH}}=\eta_{\mathrm{RH}}>0$. Thus, the sign of the intrinsic impedance is still positive in a LHM,

$$\eta=+\sqrt{\frac{\mu}{\varepsilon}}>0. \tag{4}$$

Finally, as an immediate consequence of Snell's law ($n_1\sin\theta_i=n_2\sin\theta_t$), energy is refracted on the same side of the normal as the incident wave, which means that the transmission angle is negative ($\theta_t<0$), as shown in Fig. 3.

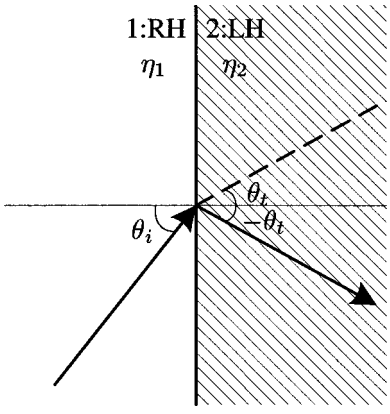

FIG. 3. Interface RH/LH with a negative angle of refraction.

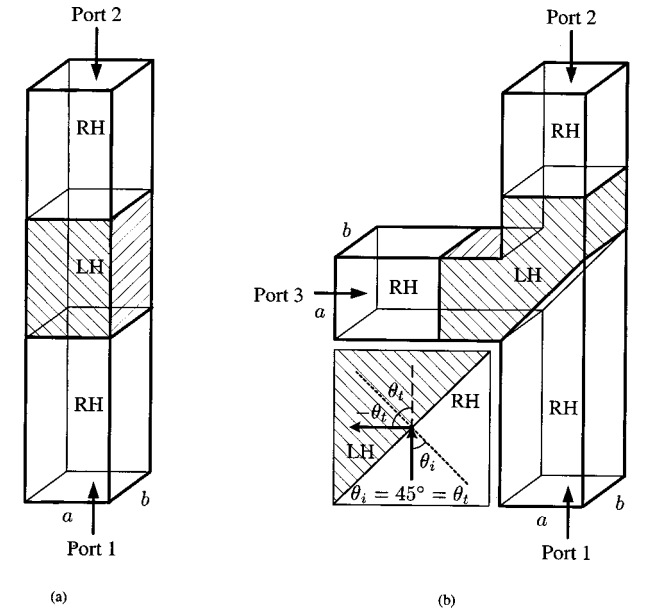

FIG. 4. LHM-loaded rectangular waveguide configurations used to verify the properties of LHMs. (a) Waveguide section. (b) T junction ($n_{\mathrm{LH}}=-n_{\mathrm{RH}}$).

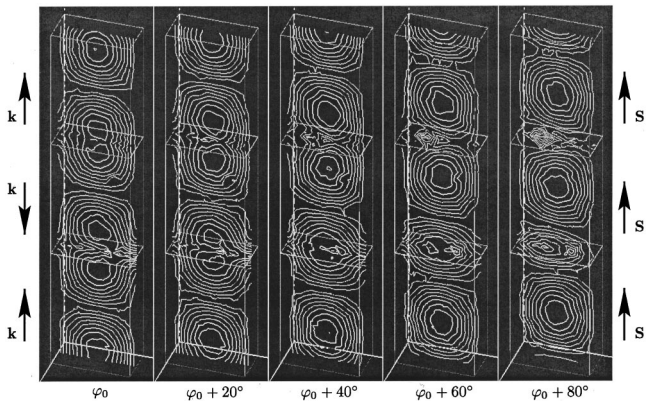

FIG. 5. Contour lines of the TE_{10}-mode **E** field ($f=1.2$ GHz) in the midplane perpendicular to the b side of the waveguide in Fig. 4(a), verifying the negative phase velocity in a LHM. The phase step between the different snapshots is $\Delta\phi=20°$.

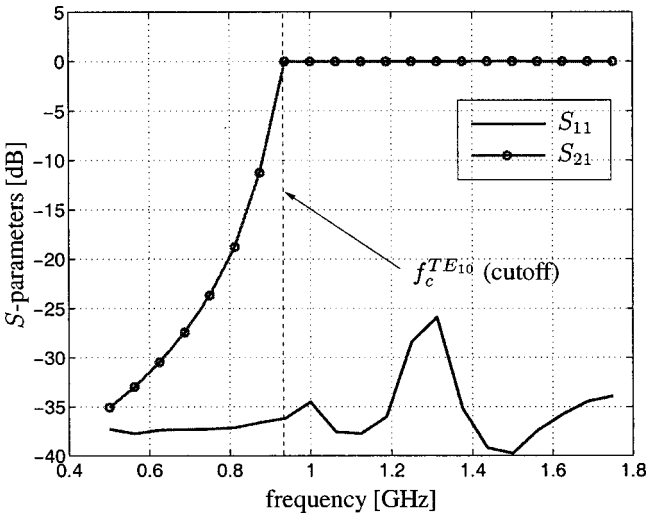

FIG. 6. S parameters for the waveguide in Fig. 4(a), verifying the perfect matching ($S_{21}=0$ dB) between a RH and of LH medium when $(\varepsilon_{r\mathrm{LH}},\mu_{r\mathrm{LH}})=-(\varepsilon_{r\mathrm{RH}},\mu_{r\mathrm{RH}})$.

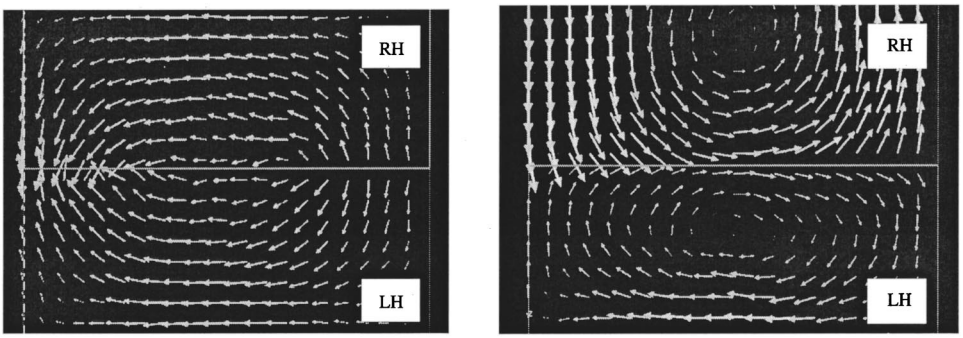

FIG. 7. TE_{10}-mode **H**-field vector ($f=1.2$ GHz) near the interface of RH/LH in Fig. 4(a), verifying the change of sign in the normal components and the continuity of the tangential components of the fields at an interface of RH/LH. (a) $\mu_{rRH}=+1$, $\mu_{rLH}=-1$; (b) $\mu_{rRH}=+1$, $\mu_{rLH}=-3$.

III. METHODOLOGY

We will verify by full-wave simulations the properties of LHMs described in Sec. II using the rectangular waveguide structures presented in Fig. 4. To do this, we used finite-element method (FEM) commercial software Ansoft-HFSS. The basic idea is to load the waveguide with a judiciously positioned and tailored LHM, and to adopt an *effective medium approach*, assuming constant negative values of ε and μ in order to clearly emphasize the fundamental effects. The effective medium approach is fully justified by the fact that LHMs operate in the long-wavelength regime (instead of the Bragg regime like photonic crystals), where the average distance between the diffraction sites or period (if the microstructure is periodic) a is much smaller than the wavelength ($a \ll \lambda$).[4,6] On the other hand, the constant ε and μ assumption is true only in a narrow frequency range in practice, since the conservation of energy requires that a LHM be dispersive.[1,7]

The configuration of Fig. 4(a) will be used to demonstrate the negative phase velocity [justifying Eq. (3)], perfect matching for $(\varepsilon_{rLH},\mu_{rLH})=-(\varepsilon_{rRH},\mu_{rRH})$ [justifying Eq. (4)] and modified BCs at an interface of RH/LH, while the configuration of Fig. 4(b) will be used to demonstrate the negative angle of refraction [further justifying Eq. (3) through Snell's law].

IV. FEM RESULTS

In the following results, the waveguide sections of Fig. 4(a) are WR-650 ($a=6.5$ in., $b=3.25$ in.) waveguides operating in their dominant TE_{10} mode. When not otherwise stated, $\varepsilon_{rRH}=\mu_{rRH}=+1$ and $\varepsilon_{rLH}=\mu_{rLH}=-1$, for which $n_{RH}=+1$, $n_{LH}=-1$.

Figure 5 shows that the wave fronts in the LH material propagate toward the source and verifies thereby the fact that $v_\varphi<0$ or, equivalently, that $n<0$. We also verified that the Poynting vector points in all regions, including the LHM region, in the direction of the propagation of energy, that is, from port 1 (input) to port 2 (output).

The S parameters for the same structure, presented in Fig. 6, demonstrate the perfect matching at an interface RH/LH when $(\varepsilon_{rLH},\mu_{rLH})=-(\varepsilon_{rRH},\mu_{rRH})$: the insertion loss is 0 dB in the whole frequency range of the TE_{10} mode.

In Fig. 7, we verify in a qualitative manner the tangential/normal BCs on the **H** field shown in Fig. 2. We also verified (not shown) the continuity of E_t in the TE_{10} mode and the sign reversal and discontinuity of E_n in the TM_{01} mode. This cannot be seen in the transverse electric (TE) modes since $E_{nTE}=0$. However, in order to remain in the dominant mode below the cutoff of higher order modes, we can replace the electric (PEC) walls of the waveguide by magnetic (PMC) walls. Then the structure is the twin of its predecessor and the **E** field of the new dominant mode, which is TM_{10}, displays features similar to the ones in Fig. 7 for the **H** field in the metallic waveguide.

Finally, Fig. 8 provides an indirect but vivid demonstration of the negative angle of refraction at a RH/LH interface. When the T junction is empty, the largest part of power is transmitted to port 2 ($S_{21}>-5$ dB) and a smaller part of it couples to port 3 ($-20<S_{31}\leqslant -5$ dB). In contrast, when the

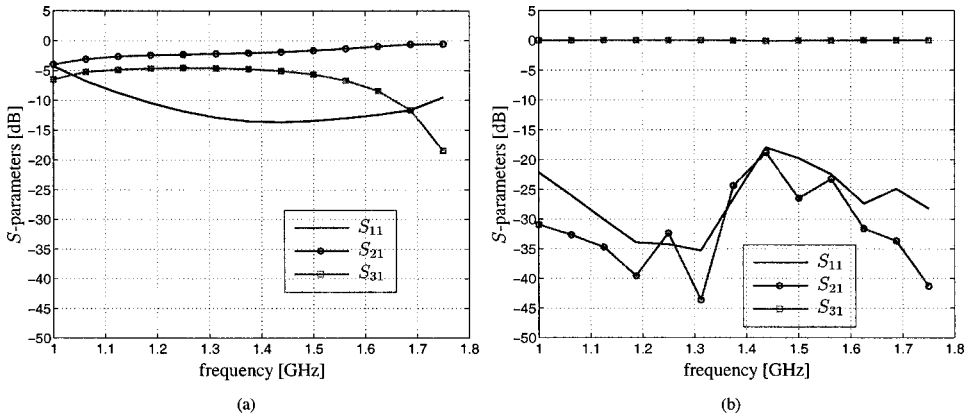

FIG. 8. S parameters for the T junction in Fig. 4(b), verifying the negative angle of refraction at a RH/LH interface ($n_{LH}=-n_{RH}$) (TE_{10}-mode frequency range). (a) Without the LH load (empty structure). (b) With the LH load.

junction is loaded by a LH material in the geometry indicated in the inset of Fig. 4(b), then *all* the power is transmitted to port 3 ($S_{31} \approx 0$ dB). This demonstrates that energy is bent by the oblique edge of the LHM by an angle of 90°, or $-45°$ with respect to the normal, in agreement with Snell's law for $n_{LH} = -n_{RH}$.

V. CONCLUSIONS

The fundamental electromagnetic properties of LHMs were reviewed and verified by full-wave analysis using waveguide structures loaded by a LHM and adopting an effective medium approach. These properties are the negative phase velocity and refractive index, the positive intrinsic impedance, the modified boundary conditions at an interface with a RH material, and the negative angle of refraction at such an interface. In addition, future developments of novel waveguide multiports with unique characteristics can be predicted from the original results presented in the case of the *T* junction.

ACKNOWLEDGMENT

The authors wish to thank Dr. Richard Remski of Ansoft Corporation for excellent technical support.

[1] V. G. Veselago, Sov. Phys. Usp. **10**, 509 (1968).
[2] J. B. Pendry, A. J. Holden, W. J. Stewart, and I. Youngs, Phys. Rev. Lett. **76**, 4773 (1996).
[3] J. B. Pendry, A. J. Holden, and W. J. Stewart, IEEE Trans. Microwave Theory Tech. **47**, 2075 (1999).
[4] R. A. Shelby, D. R. Smith, and S. Schultz, Science **292**, 77 (2001).
[5] J. B. Pendry, Phys. Rev. Lett. **85**, 3966 (2000).
[6] D. R. Smith, W. J. Padilla, D. C. Vier, S. C. Nemat-Nasser, and S. Schultz, Phys. Rev. Lett. **84**, 4184 (2000).
[7] D. R. Smith and N. Kroll, Phys. Rev. Lett. **85**, 2933 (2000).